Energy Advances

ROYAL SOCIETY OF CHEMISTRY

PERSPECTIVE

View Article Online
View Journal | View Issue

Cite this: *Energy Adv.*, 2023, 2, 606

The role of graphene in new thermoelectric materials†

Rafiq Mulla, *[a] Alvin Orbaek White, [a] Charles W. Dunnill[ab] and Andrew R. Barron*[acde]

Graphene has high electrical conductivity, making it an attractive material for thermoelectric applications. However, its high thermal conductivity is a major challenge, and initial studies indicate that using pristine graphene alone cannot achieve optimal thermoelectric performance. Therefore, researchers are exploring ways to improve thermoelectric materials by either leveraging graphene's high intrinsic electrical conductivity or compounding graphene with additives to reduce the intrinsic thermal conductivity of the materials. Therefore, the research focus is now being shifted to graphene composites, primarily with polymer/organic conductors. One promising avenue of research is the development of graphene composites with polymer or organic conductors, which have shown some improvements in thermoelectric performance. However, the achieved "dimensionless figure of merit (*ZT*)" values of these composites are still far lower than those of common inorganic semiconductors. An alternative approach involves incorporating a very small amount of graphene into inorganic materials to improve their overall thermoelectric properties. These new concepts have successfully addressed the detrimental effects of graphene's intrinsic thermal conductivity, with the added interfaces in the matrix due to the presence of graphene layers working to enhance the properties of the host material. The use of graphene presents a promising solution to the longstanding challenge of developing high-performance and cost-effective thermoelectric materials. This paper discusses these innovative research ideas, highlighting their potential for revolutionizing the field of thermoelectric materials.

Received 22nd February 2023,
Accepted 22nd March 2023

DOI: 10.1039/d3ya00085k

rsc.li/energy-advances

1. Introduction

Climate change has brought energy systems into the spotlight, and energy sourcing has become a common topic across the sciences, politics, global finance, and industry.[1,2] One attractive step towards mitigating excess energy loss and decreasing emissions of greenhouse gases is the conversion of thermal energy from waste heat, which can replace fossil fuel energy sources that would otherwise contribute to the changing climate.[3] Thermoelectric materials can effectively convert thermal energy into electrical energy and *vice versa*.[4,5] The conversion of thermal energy to electrical energy using thermoelectric materials is measured and compared based on their "dimensionless figure of merit" (*ZT*).[2,6] A large figure of merit is desirable for the thermoelectric conversion process between thermal transfer and electrical transfer within the materials; however, as both transfer mechanisms typically rely on identical physical entities such as electron and phonons, it is challenging to increase one transfer process without also increasing the other.[7] As a consequence, there is often an intrinsic trade-off between increasing thermal conduction and/or the electrical conduction of the materials. Recent advances aim to increase one transfer mechanism over the other to create materials with a larger figure of merit or power factor, enabling more effective harvesting of electrical energy from waste heat. The heat-to-electricity conversion efficiency of a device depends on the material's *ZT*, described in eqn (1), where S, σ, κ, and T are the Seebeck coefficient, electrical conductivity, thermal conductivity, and, the absolute temperature, respectively.[8]

$$ZT = \frac{S^2\sigma T}{\kappa} \quad (1)$$

An efficient thermoelectric material should have excellent electrical conductivity, high Seebeck coefficient, and low thermal conductivity.[9] The last few decades have witnessed significant progress in thermoelectric research with continuous breakthroughs in *ZT* using the best performing materials such

[a] *Energy Safety Research Institute, Swansea University, Bay Campus, Swansea, SA1 8EN, UK. E-mail: a.r.barron@swansea.ac.uk, rafiq.mulla@swansea.ac.uk*
[b] *Ceres Power Limited, Horsham, England, UK*
[c] *Arizona Institute for Resilient Environments and Societies (AIRES), University of Arizona, Tucson, AZ 85721, USA*
[d] *Department of Chemistry and Department of Materials Science and Nanoengineering, Rice University, Houston, TX 77005, USA*
[e] *Faculty of Engineering, Universiti Teknologi Brunei, Brunei Darussalam, Brunei*
† Electronic supplementary information (ESI) available. See DOI: https://doi.org/10.1039/d3ya00085k

as Bi_2Te_3, PbTe, and SiGe;[10] however, just as these inorganic materials have gained momentum in recent years so have concerns regarding both the scarcity and toxicity of these materials.[11] Therefore, the development of less-toxic and lower-cost thermoelectric materials has been a major research topic in the field. Careful optimisation of the thermoelectric properties is extremely important to achieve high *ZT*; however, independent control of the electrical and thermal properties is one of the trickiest and most challenging issues.[12] Various new strategies such as nano-structuring and composite formations are gaining increased interest and thus different and new materials have been developed in the last few decades.[10]

The first-generation thermoelectric materials had low power conversion efficiencies of 3–6%, while new materials can achieve efficiencies of 12–15%.[13] This represents a significant improvement in converting heat energy into electricity, making it commercially viable for various applications. Recent advancements in thermoelectric research include the discovery of new materials with high thermoelectric efficiency, such as skutterudites and half-Heusler compounds,[14–16] and improving the efficiency of thermoelectric materials through nanostructuring,[10,17] doping,[18] band engineering,[7] and structural manipulations.[19–23] Thermoelectric materials have potential applications in various industries, including automotive, electronics, and aerospace, by recovering waste heat and powering sensors and other low-power devices.[24–27] These advancements offer opportunities for developing more efficient and sustainable energy technologies.

Graphene is a two-dimensional carbon lattice has excellent electrical and thermal properties.[28] After graphene's discovery as the best electricity and heat conductor, there was a rapid increase in the interest from researchers to explore its thermoelectric properties. Although graphene has ultrahigh carrier mobility (15 000 $cm^2\ V^{-1}\ s^{-1}$) which is responsible for its excellent electrical conductivity, the extremely high thermal conductivity of graphene (that could be up to 2500 to 5000 $W\ m^{-1}\ K^{-1}$) is a major drawback to be used as a thermoelectric element.[29,30] In addition, graphene's low Seebeck coefficient (typically reported values are in the range of 10 to 100 $\mu V\ K^{-1}$) makes it difficult to achieve a useful thermoelectric voltage generation.[31,32] Due to all these factors, the reported *ZT* values for pristine graphene are extremely low which are of the order of $\sim 10^{-4}$ except in a few recent studies. For example, in suspended graphene nanoribbons of width $\sim$40 nm and length $\sim$0.25 micron, a record high *ZT* of 0.1 has been observed;[33] whereas a typical semiconductor exhibits a decent *ZT* of 1 to 2.[29,34,35]

Shortly after the discovery of graphene, it was realized that despite its excellent electrical conductivity in pristine form, it is unsuitable for thermoelectrics mainly due to its inherent thermal conductivity. Therefore, the focus has shifted towards using graphene in the fabrication of composites, mostly with polymers or organic conductors. The primary aim was to improve the electrical conductivity of the polymeric/organic matrix or to reduce the thermal conductivity of the graphene itself.[36–39] Despite initial improvements, the achieved *ZT* values were still low as compared to common inorganic semiconductors, which have very low thermal conductivity and good Seebeck coefficients and are thus the best candidates for thermoelectric applications. However, the conversion efficiency of thermoelectric devices is still poor, and further enhancement in the *ZT* is needed to extend their use to different practical applications. Many strategies, such as impurity doping, alloying, resonant level doping, nanostructuring, and defect creation, have been used extensively to improve the performances of existing thermoelectric materials.[40] Almost all the semiconductors that are considered good thermoelectric materials have better *ZT* than pristine graphene, yet graphene is attractive due to its excellent electrical properties compared to semiconductors. Researchers have used graphene as an additive for the host inorganic material, which has yielded promising results.[1,16,41–44] The enhancements in the thermoelectric properties have been attributed to different possible mechanisms, such as carrier or energy filtering effects, increased boundary scattering of long-wavelength phonons, and increased carrier mobility.[45]

Despite the wide variety of experimental conditions that have been used there was on common thread throughout, in all of these research studies, a very small fraction of graphene has been used as an additive in the bulk matrix; and this was enough to enhance the thermoelectric properties. As discussed, thermoelectric research on graphene can be grouped into two of which the majority of the initial studies are dominated by graphene–polymer/organic-based composites and a few recent works are on graphene–inorganic semiconductor based composites in which promising and competitive performances have been observed.

2. Graphene–polymer/organic composites

Substantial research has been carried out on polymers/organic compounds such as polyaniline (PANI), poly(3,4-ethylenedioxythiophene)poly(styrenesulfonate) (PEDOT:PSS), polypyrrole (PPy), polyacetylene (PA), polythiophene (PTH), (the chemical structures of these polymers are provided in the ESI†) to explore and use them for thermoelectric applications as these materials possess very low thermal conductivity which is an important aspect to achieve better thermal gradients across the thermoelectric devices.[46–51] In addition, these polymers are very beneficial to fabricating flexible devices,[50,52–54] but most of these compounds have low levels of electrical conductivity and/or low Seebeck coefficient, which result in low power factor ($S^2\sigma$) and the *ZT*.[29,55] Many different hybrid composites have been fabricated by incorporating graphene into polymer/organic species through covalent and/or non-covalent interactions.[47,56] Different preparation methods such as powder mixing, *in situ* polymerization, solution dispersion, and layer by layer deposition are in practice to produce this type of composites.[29,57–59] In general, a simple mechanical mixing is routinely used which gives desired composite matrix and the content of graphene in the polymer matrix is systematically varied to see the changes in the thermoelectric properties of the resulting composites. A schematic illustration showing the typical structure of these graphene containing polymer/organic matrix is given in Fig. 1. It is

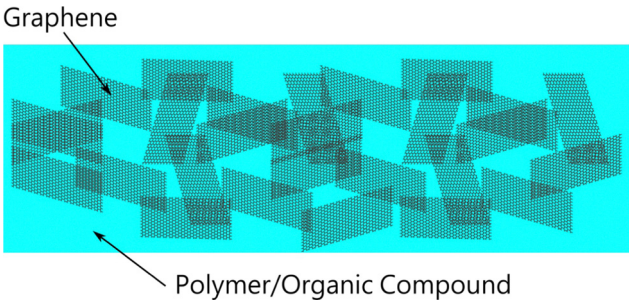

Fig. 1 Schematic diagram of graphene–polymer/organic hybrid composites.

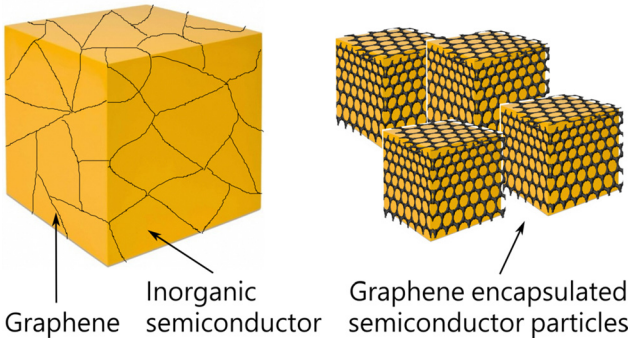

Fig. 2 Schematic diagram of inorganic semiconductor/graphene composite and graphene encapsulated nano/micron sized grains/particles.

more than a physical mixing of the polymer and graphene where the enhancements in the properties are attributed to the strong π–π coupling interactions between polymer and graphene.[29]

The PEDOT:PSS-Graphene nano-composite thin film showed significant improvements in the electrical conductivity from 0.74 S cm^{-1} (for pure PEDOT:PSS) to 32.13 S cm^{-1} (2 wt% graphene in PEDOT:PSS) and power factor from 2 to 11 μW m^{-1} K^{-2} which resulted in the enhancement of *ZT* from 2.0×10^{-3} to 2.1×10^{-2} (at room temperature); an order of magnitude improvement in the thermoelectric performance.[55] Similarly, a PANI/graphene film prepared by a solution dispersion method produced a better power factor of 19 μW m^{-1} K^{-2} which is again attributed to the improved electrical conductivity of the film due to the addition of graphene.[60] Improvements in the graphene–organic composites have also been realized by further doping them with different materials; for example, camphorsulfonic acid (CAS) doped PANI/reduced graphene oxide (rGO) films have produced a very high electrical conductivity of 3677 S cm^{-1} as compared to the undoped ones and resulted in a promising power factor of 214 μW m^{-1} K^{-2};[61] however, most of the reported power factors or *ZT* values achieved are far lower than the typical values achieved in case of inorganic semiconductors and also they are thermally not stable due to the presence of organic/polymer compounds.

3. Graphene–inorganic semiconductor composites

In the case of graphene–inorganic semiconductor composites, graphene layers are introduced into the inorganic matrix either by solid-state mixing or by liquid-state mixing.[29] Both of these methods are simple but solid-state mixing gives better control over composition than liquid-state mixing. In solid-state mixing, both graphene and inorganic compounds are in solid powder form and traditional ball milling or mechanical grinding is used to obtain composites whereas, in liquid-state mixing, either both or one of them will be in the form of a solution and composites are obtained by stirring or hydrothermal method.[29] Here, a uniform distribution of graphene into the host matrix is very important in order to see the changes in the properties which require a long time milling or grinding of the mixtures. Better outputs were observed when graphene layers are uniformly distributed into the matrix or encapsulate the inorganic host particles as illustrated in Fig. 2. In such graphene added matrix, there is a possibility of optimizing the electrical properties of the composite that could be associated with increased charge carrier mobility due to the presence of graphene in the matrix, phonon scattering due to interfaces between the graphene and host particle surfaces, energy filtering effect that again arises from the graphene/matrix interfaces where the two different Fermi levels meet and result in band bending. Improvements in the thermoelectric performance of different materials have been observed experimentally and a common observation from the majority of the studies suggests that the presence of graphene in the composite matrix improves electrical conductivity alongside reducing thermal conductivity which results in enhanced *ZT* of the materials (Fig. 3). In polycrystalline materials, the trapped charges at the grain boundaries influence charge carrier movements as there is the formation of electrostatic potential barriers between the grains because of which low energy charges often scatter back and affect the electrical conductivity.[62] Graphene layers between the grain boundaries are thought to be reducing the potential barrier; thereby improvements can be achieved in the electrical conductivity. According to the predicted mechanism for the reduced thermal transport, there is a mismatch between the phonon density of states of graphene and the host inorganic compound at the grain boundaries which depresses phonon transport across the inhomogeneous microstructures.[42]

Further, depending on the work functions of graphene and the host matrix, the effect of graphene at the interfaces can be optimised based on the possible band alignment at the graphene–matrix interfaces.[63] As illustrated by Fig. 4, Schottky barriers occur at the interfaces for both n- and p-type semiconductors.[63] In such incidents, the generated potential barrier (Eb) can preferentially scatter low energy charge carriers resulting in carrier filtering. Whereas there is no potential barrier from Ohmic contact and thus all carriers can pass the interface (Fig. 4c and d). However in such cases, charges may experience scatterings due to potential energy variations between the graphene and matrix. Therefore, graphene–matrix interfaces can provide an effective way for energy filtering, which helps modify thermoelectric properties of the resulting compounds.

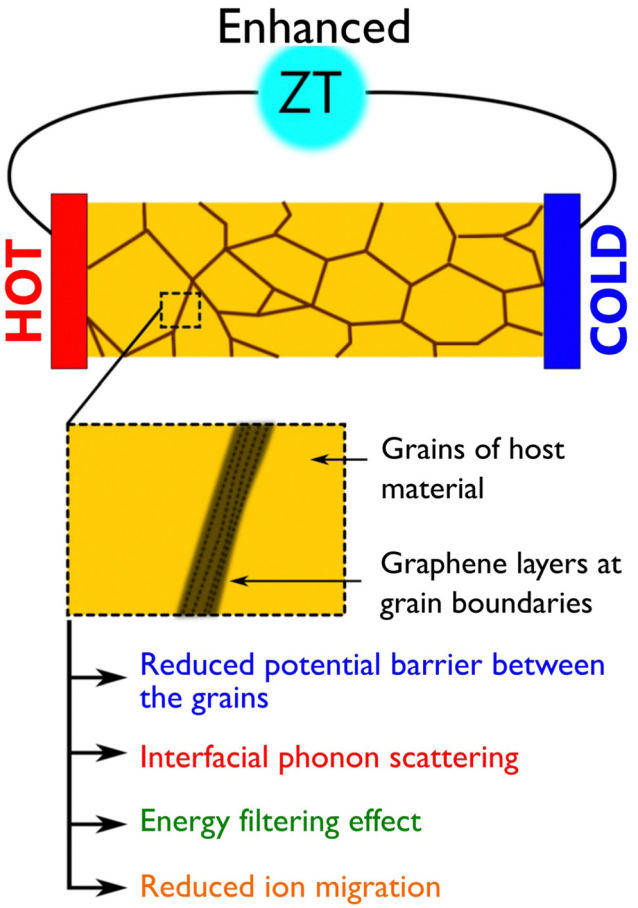

Fig. 3 An illustration showing the factors that are responsible for the enhancement of *ZT* in graphene based inorganic composites.

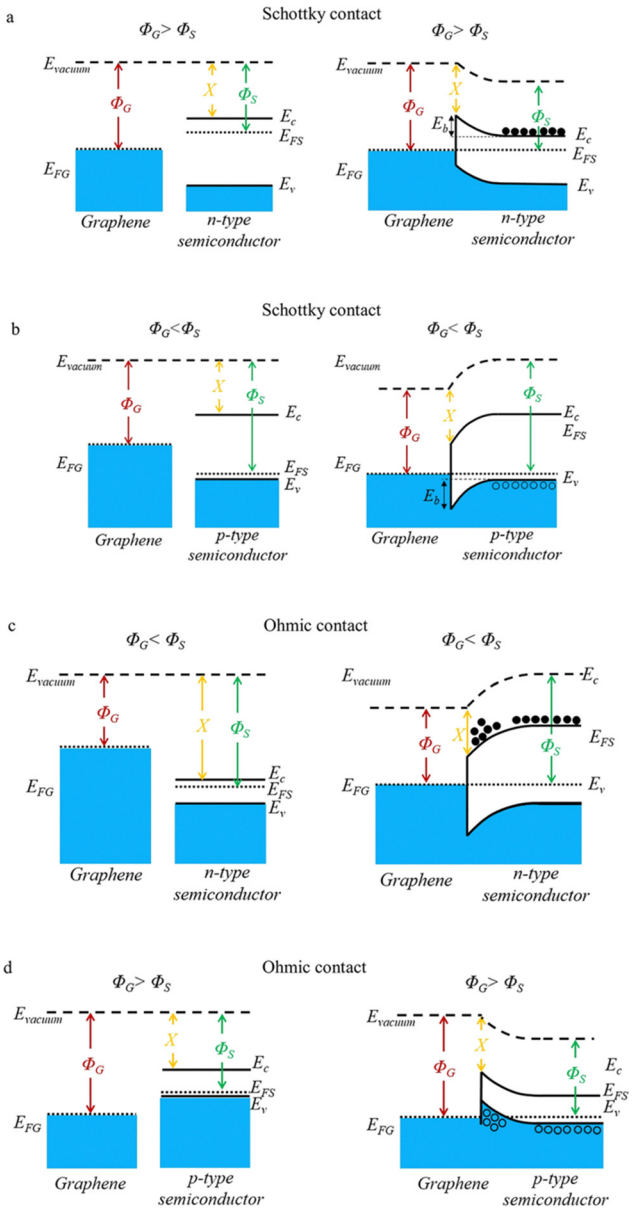

Fig. 4 Schematic illustrations of different contacts and band alignments at the graphene–matrix interface. Schottky contact for graphene/n-type (a) and graphene/p-type semiconductor(b), Ohmic contact for graphene/n-type (c) and graphene/p-type semiconductor(d). (Φ_G-graphene work function; Φ_S-semiconductor work function). Reproduced with permission from Ref. 63 Copyright 2021, American Chemical Society.

In addition, graphene encapsulation on the grains/particles can act as a protecting layer that controls/blocks the ion migration (ion migration is a major problem in some thermoelectric materials which deteriorates their thermoelectric performance over repeated use).[64] As illustrated in Fig. 5a, the layer like nature of graphene easily encapsulates the particles during the synthesis process and several experiments have observed the presence of graphene on the grain boundaries (Fig. 5b and c).

It is also observed that addition of graphene into the matrix can improve the mechanical and thermal stability properties without deteriorating thermoelectric properties of the composite material (Fig. 6).[63,65] Numerous studies have demonstrated that the improved mechanical properties of thermoelectric materials with added graphene are a result of the strengthening impact of hierarchically structured graphene and reduced grain size. Incorporating graphene into thermoelectric materials can improve their mechanical properties, including hardness, flexibility, and tensile strength.[63,66,67] This enhancement can make the materials more durable and reliable for various thermoelectric applications, although the optimal graphene content and distribution need to be carefully managed.

Further, graphene-based composites can affect the carrier concentration and mobility in several ways, including introducing additional charge carriers into the material and improving carrier mobility by providing a conductive path. Optimizing these properties through the use of graphene-based composites can enhance the thermoelectric performance of the material, making it more efficient. The presence of double Schottky barriers at grain boundaries may trap some electrons and hinder their contribution to electrical conduction. Graphene has been shown to be effective in weakening the double Schottky barriers in several composites.[29] Reducing the Schottky barrier can lead to the release of trapped electrons and increased mobility, resulting in an increase in both carrier concentration and mobility. An appropriate amount of

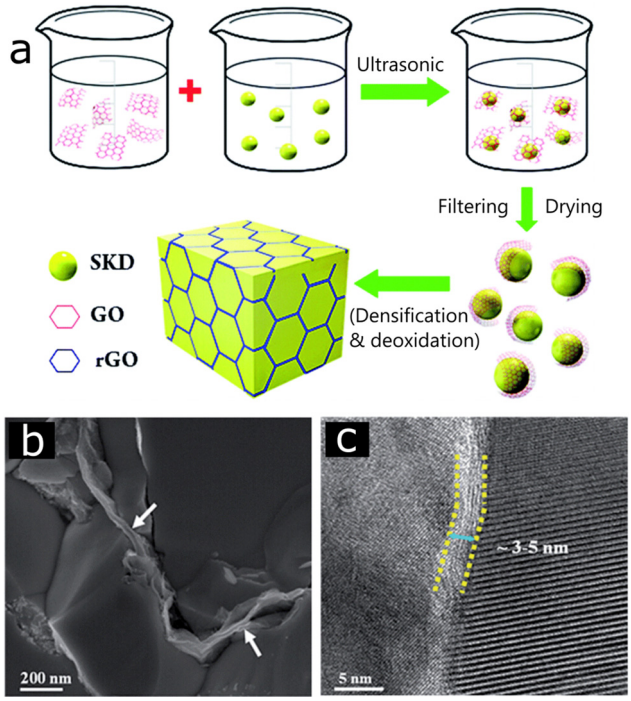

Fig. 5 (a) Schematic showing the synthesis process of the 3D-rGO network wrapping on skutterudite (SKD) particles, (b and c) SEM and TEM images of the sintered SKD/rGO surface showing rGO coating on boundaries, Reproduced with permission from Ref. 45 Copyright 2015, Royal Society of Chemistry.

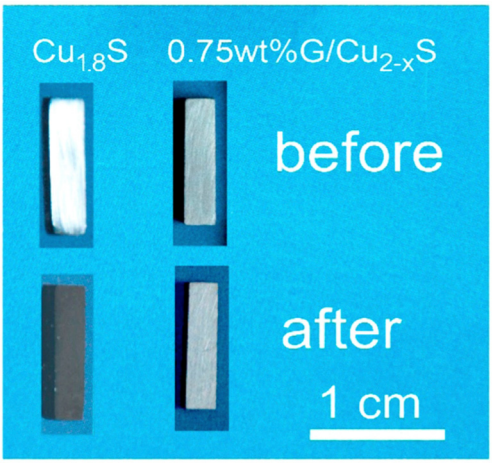

Fig. 6 Photos of the $Cu_{1.8}S$ before and after high temperature test at 723 K, and 0.75 wt% graphene/$Cu_{2-x}S$ at 873 K, respectively, Reproduced with permission from Ref. 1 Copyright 2018, Elsevier BV.

graphene can help achieve increased carrier concentration and mobility. However, excessive graphene content can lead to decreased carrier concentration and/or mobility due to interfacial carrier blocking caused by aggregated or thickened graphene.[29]

All these factors which are collectively responsible for the enhancement of *ZT* are illustrated in Fig. 3. In a recent study, a thermoelectric module having graphene added composite legs ($Ce_{0.85}Fe_3CoSb_{12}$/1.4 vol% rGO and $Yb_{0.27}Co_4Sb_{12}$/0.72 vol% rGO composite as p and n-type thermoelectric legs, respectively), a high efficiency of 8.4% and maximum power output of 3.8 W were achieved (Fig. 7a and b), which is appreciably higher than the performance of pristine skutterudite module (maximum efficiency and power output were 6.8% and 3.1 W, respectively).

Recent works on graphene incorporated copper sulfide ($Cu_{2-x}S$) and copper selenide (Cu_2Se) are the best examples to illustrate the effect of graphene on the optimisation of electronic properties.[1,42] In the case of graphene incorporated $Cu_{2-x}S$, a high power factor of 1197 μW $m^{-1}K^{-2}$and a significant *ZT* enhancement reaching up to 1.56 (at 873 K) has been observed from a sample having 0.75 wt% graphene in it; the maximum *ZT* observed for pristine samples is below 1.00 (measured at 723 K). Additionally, a peculiar characteristic of the graphene added composite samples is the decreased thermal conductivity (0.67 W m^{-1} K^{-1} at 873 K); lower than the pristine $Cu_{2-x}S$. Generally, graphene should increase the thermal conductivity of the composite but since it is in a very small amount and dispersed in a network form, it is predicted that the added interfaces and their associated strains are likely to increase the phonon scattering.[1] In addition, the study also found that the incorporation of graphene was effective to improve the thermal stability of $Cu_{2-x}S$ which was investigated and confirmed by the cyclic thermal test from room temperature to 873 K (Fig. 3c); this is an important feature when thermoelectric devices are employed for high temperature waste heat harvesting applications.

In Cu_2Se, a significant depression in the thermal conductivity was achieved by adding 0.8 wt.% carbon nanodots into it which resulted in a high *ZT* of 1.98 at 973 K,[68] in a similar approach from the addition of 0.15 wt% graphene nanoplates, an ultrahigh *ZT* of 2.44 at 870 K was achieved, which is one of the highest *ZT* achieved in graphene incorporated composites; illustrating graphene's potential as an additive.[42] The study suggested that the reduction of thermal conductivity was from a frequency mismatch in the phonon density of states between Cu_2Se and carbon honeycomb. Recently, Wang *et al.* produced a series of Ag_2Se/carbon nanotubes nanocomposites and tuned the concentration of carbon nanotubes to effectively optimize the transport and mechanical properties of the composites. They achieved an enhanced *ZT* of 0.97 at 375 K with 0.5 wt% of carbon nanotubes as the optimized addition amount.[69] Similarly, Zhao *et al.* demonstrated significantly enhanced *ZT* of Cu_2Se from the incorporation of a small weight fraction of carbon from various carbon sources. Several carbon-added Cu_2Se composites exhibited enhanced *ZT* values with a maximum achieved *ZT* of ~2.4 at 850 K.[70]

Another study has observed a significant reduction in the thermal conductivity of a skutterudite material ($Yb_yCo_4Sb_{12}$) by synthesizing micron-sized $Yb_yCo_4Sb_{12}$ grains wrapped in graphene layers, resulting in a high *ZT* of 1.5.[16] In a similar work, carbon-encapsulated copper sulfide showed a 13% enhancement in *ZT*, with a maximum of 1.04 at 773 K.[71] Graphene has also been used to form composites with electrically less conducting materials such as TiO_2 and Fe_2O_3, improving their thermoelectric properties by creating conducting pathways for charge carriers through the layered structure of graphene.[12,72,73] Numerous

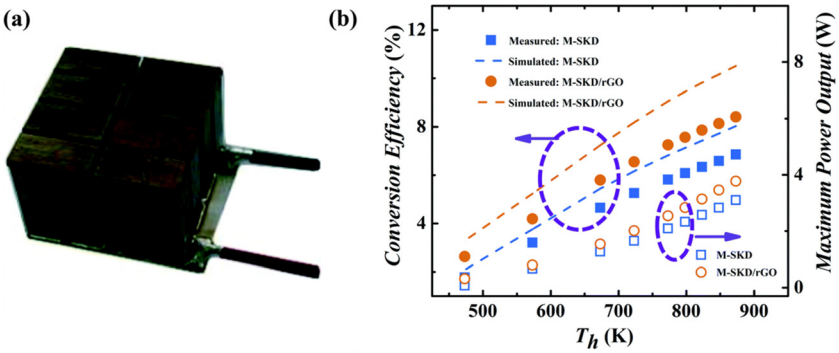

Fig. 7 A thermoelectric module (dimension of 20 mm × 20 mm × 16 mm) designed using $Ce_{0.85}Fe_3CoSb_{12}$/1.4 vol% rGO and $Yb_{0.27}Co_4Sb_{12}$/0.72 vol% rGO composite as p and n-type thermoelectric legs, respectively, and its (*f*) conversion efficiency and power outputs as a function of hot side temperature (T_h) for the skutterudite/rGO based devices (M-SKD/rGO) (a reference device was made from pure SKD (M-SKD)). The dash lines represent the theoretical conversion efficiency of M-SKD/rGO and M-SKD modules. Reproduced with permission from Ref. 16 Copyright 2016, Royal Society of Chemistry.

studies of graphene-added inorganic materials have demonstrated thermoelectric enhancements, as summarized in Fig. 8 and Table 1. In each case, the difference between the pristine material and the material with graphene additive is positive, indicating an improvement in *ZT*. This trend in enhancing *ZT* has been observed across a wide range of inorganic materials.

4. Summary and outlook

As the need for recycling waste heat from various sources and cooling applications grows increasingly critical for the future, the importance of thermoelectric materials with good conversion efficiency becomes ever more apparent. The research on graphene-based materials is rapidly expanding, and recent efforts have yielded admirable progress. Achieving a uniform distribution or encapsulation of graphene on nano/microscale particles/grains is essential to bring about significant changes in properties. Despite graphene's extremely high thermal conductivity, its incorporation plays a significant role in reducing the thermal conductivity of many thermoelectric materials, as shown in the literature.

Here are a few potential research directions for graphene-incorporated thermoelectric composites:

- The effect of different types of graphene, such as monolayer, bilayer, or multilayer graphene, on the thermoelectric properties of the composite.
- Exploring the thermoelectric characteristics of heterostructures based on graphene, where graphene is combined with other materials. These heterostructures can be created by incorporating transition metal dichalcogenides, such as MoS_2 or WSe_2, into the graphene framework to produce composites with enahanced thermoelectric properties.
- Investigating semiconductor/graphene core/shell nanostructures of varying combinations and particle sizes could lead to the discovery of novel thermoelectric composites that exhibit superior performance.

It is also worth noting that the size of graphene can influence the thermoelectric performance of materials. Numerous studies have shown that thin layers of graphene are more beneficial than thick ones, making the use of high-quality few-layer or monolayer graphene essential to enhance the thermoelectric properties of composites. Graphene's electrical and thermal properties depend heavily on its size, shape, and structure. Therefore, when

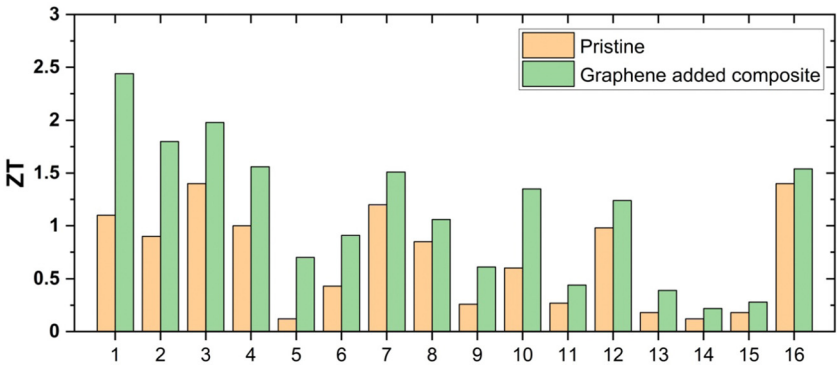

Fig. 8 Thermoelectric *ZT* values of pristine and graphene-added composites, (1) Cu_2Se/graphene,[42] (2) Cu_2Se/graphene,[74] (3) Cu_2Se/carbon,[68] (4) $Cu_{2-x}S$/graphene,[1] (5) PbTe/graphene,[75] (6) SnSe/rGO,[76] (7) $YbyCo_4Sb_{12}$/rGO,[16] (8) $Ce_{0.85}Fe_3CoSb_{12}$/rGO,[16] (9) $CoSb_3$/graphene,[77] (10) $Mg_3Sb_{1.8}Bi_{0.2}$/graphene,[78] (11) Cu_2SnSe_3/graphene,[79] (12) $Bi_{0.5}Sb_{1.5}Te_3$/graphene,[80] (13) $Bi_{85}Sb_{15}$/graphene,[81] (14) $SrTiO_3$/rGO,[82] (15) Al–ZnO/rGO,[83] (16) BiSbTe/graphene.[84]

Table 1 Thermoelectric *ZT* achieved in different graphene incorporated materials

Composite material	Graphene/Carbon content in the composite	*ZT* for pristine material	*ZT* after graphene incorporation	Enhancement (%)	Ref.
Cu_2Se/graphene composite	0.15 wt%	1.10	2.44	121	42
Cu_2Se/graphene composite	0.25 wt%	0.90	1.80	100	74
Cu_2Se/carbon nanodots composite	0.80 wt%	1.40	1.98	41	68
Ag_2Se/carbon nanotubes composites	0.5 wt%	0.74	0.97	31	69
Carbon-reinforced Cu_2Se nanocrystalline solids	0.3 wt%	1.40	2.40	71	70
$Cu_{2-x}S$/graphene composite	0.75 wt%	1.00	1.56	56	1
PbTe/graphene nanocomposite	3.00 wt%	0.12	0.70	483	75
SnSe/rGO nanocomposite	0.30 wt%	0.43	0.91	111	76
$Yb_yCo_4Sb_{12}$/rGO composite	0.72 vol%	1.20	1.51	25	16
$Ce_{0.85}Fe_3CoSb_{12}$/rGO composite	1.40 vol%	0.85	1.06	24	16
$CoSb_3$/graphene nanocomposite	1.50 wt%	0.26	0.61	134	77
$Mg_3Sb_{1.8}Bi_{0.2}$/graphene nanocomposite	1.25 wt%	0.60	1.35	125	78
Cu_2SnSe_3/graphene composites	0.25 vol%	0.27	0.44	62	79
$Bi_{0.5}Sb_{1.5}Te_3$/expanded graphene composites	0.10 vol%	0.98	1.24	26	80
$Bi_{85}Sb_{15}$/graphene composite	0.50 wt%	0.18	0.39	116	81
$SrTiO_3$/rGO composite	0.60 wt%	0.12	0.22	83	85
Al–ZnO/rGO composite	1.50 wt%	0.18	0.28	55	83
$SrTiO_3$/rGO composite	0.64 vol%	0.03	0.09	200	82
BiSbTe/Graphene composites	0.40 vol%	1.40	1.54	10	84

incorporating graphene into thermoelectric materials, the size and shape of the graphene layers/particles can significantly impact the overall thermoelectric performance of the composite material. For instance, the width of graphene nanoribbons has a direct correlation with their thermal conductivity, whereby the thermal conductivity increases as the width of the nanoribbon increases.[30,86,87] Conversely, the thermal conductivity of graphene nanoribbons decreases with increasing edge roughness.[86] Further research is needed to fully explore the role of graphene size in thermoelectric composites.

Graphene's robust nature and reasonably inert properties enable its use in any type of composite synthesis process, such as mechanical milling or solution-based synthesis, without much degradation of its electrical properties. However, graphene layers can be readily functionalized with organic molecules that may alter its electrical properties.[65,88,89] These changes can be remedied using simple annealing or sintering processes. Conversely, graphene's layer-like structure can be the best coating material for semiconductor grains or particles on both the nano and micro scales to improve their thermal stability for high-temperature material applications. Moreover, the *ZT* values achieved in the graphene added low-cost and less/non-toxic inorganic compounds such as Cu_2S and Cu_2Se have competitive performances contrasting with toxic and expensive tellurium-based compounds. Further rigorous investigations may yield more good news on cost-effective and environmentally friendly thermoelectrics. Based on the majority of research studies published on graphene-incorporated materials, it is clear that while graphene may not be the sole solution, it has the potential to significantly enhance the performance of thermoelectric devices as a major contributor.

Author contributions

Rafiq Mulla: conceptualization, visualization, writing – original draft. Alvin Orbaek White: writing – review & editing, supervision. Charles W. Dunnill1: writing – review & editing, supervision. Andrew R. Barron: writing – review & editing, funding acquisition, project administration, supervision.

Conflicts of interest

There are no conflicts of interest to declare.

Acknowledgements

Authors are thankful to the Welsh Government (EU European Regional Development Fund) for funding the RICE (Reducing Industrial Carbon Emission) project (Grant Number: 81435), and for funding AOW as Sêr Cymru II Fellow and Welsh Government Capital Fund (Grant number: 290).

References

1 H. Tang, F.-H. Sun, J.-F. Dong, Asfandiyar, H.-L. Zhuang, Y. Pan and J.-F. Li, *Nano Energy*, 2018, **49**, 267–273.
2 R. Matsumoto, *Carbon*, 2016, **104**, 264.
3 N. Jaziri, A. Boughamoura, J. Müller, B. Mezghani, F. Tounsi and M. Ismail, *Energy Rep.*, 2020, **6**, 264–287.
4 M. R. Burton, T. Liu, J. McGettrick, S. Mehraban, J. Baker, A. Pockett, T. Watson, O. Fenwick and M. J. Carnie, *Adv. Mater.*, 2018, **30**, 1801357.
5 Y. Du, J. Chen, Q. Meng, Y. Dou, J. Xu and S. Z. Shen, *Vacuum*, 2020, **178**, 109384.
6 P. A. Finn, C. Asker, K. Wan, E. Bilotti, O. Fenwick and C. B. Nielsen, *Front. Electron. Mater.*, 2021, **1**, 677845.
7 R. Mulla and C. W. Dunnill, *Mater. Adv.*, 2022, **3**, 125–141.
8 Y. Zhang, J.-H. Bahk, J. Lee, C. S. Birkel, M. L. Snedaker, D. Liu, H. Zeng, M. Moskovits, A. Shakouri and G. D. Stucky, *Adv. Mater.*, 2014, **26**, 2755–2761.

9 T. A. Amollo, G. T. Mola, M. S. K. Kirui and V. O. Nyamori, *Crit. Rev. Solid State Mater. Sci.*, 2018, **43**, 133–157.
10 Z.-G. Chen, G. Han, L. Yang, L. Cheng and J. Zou, *Prog. Nat. Sci.: Mater. Int.*, 2012, **22**, 535–549.
11 R. Mulla and C. W. Dunnill, *ChemSusChem*, 2019, **12**, 3882–3895.
12 W. H. Nam, Y. S. Lim, W. Kim, H. K. Seo, K. S. Dae, S. Lee, W.-S. Seo and J. Y. Lee, *Nanoscale*, 2017, **9**, 7830–7838.
13 Q. Yan and M. G. Kanatzidis, *Nat. Mater.*, 2022, **21**, 503–513.
14 J. Ma, A. S. Nissimagoudar, S. Wang and W. Li, *Phys. Status Solidi RRL*, 2020, **14**, 2000084.
15 H. Feng, Q. Deng, Y. Zhong, X. Rao, Y. Wang, J. Zhu, F. Zhang and R. Ang, *J. Mater. Sci. Technol.*, 2023, **150**, 168–174.
16 P.-a Zong, R. Hanus, M. Dylla, Y. Tang, J. Liao, Q. Zhang, G. J. Snyder and L. Chen, *Energy Environ. Sci.*, 2017, **10**, 183–191.
17 S. S. Kubakaddi and B. G. Mulimani, *J. Appl. Phys.*, 1985, **58**, 3643–3645.
18 A. Pal, K. Shyam Prasad, K. Gurukrishna, S. Mangavati, P. Poornesh, A. Rao, Y.-C. Chung and Y. K. Kuo, *J. Phys. Chem. Solids*, 2023, **175**, 111197.
19 Z.-H. Zheng, X.-L. Shi, D.-W. Ao, W.-D. Liu, Y.-X. Chen, F. Li, S. Chen, X.-Q. Tian, X.-R. Li, J.-Y. Duan, H.-L. Ma, X.-H. Zhang, G.-X. Liang, P. Fan and Z.-G. Chen, *Nano Energy*, 2021, **81**, 105683.
20 Y.-X. Chen, X.-L. Shi, Z.-H. Zheng, F. Li, W.-D. Liu, W.-Y. Chen, X.-R. Li, G.-X. Liang, J.-T. Luo, P. Fan and Z.-G. Chen, *Mater. Today Phys.*, 2021, **16**, 100306.
21 Z. Rashid, A. S. Nissimagoudar and W. Li, *Phys. Chem. Chem. Phys.*, 2019, **21**, 5679–5688.
22 P. A. Finn, C. Asker, K. Wan, E. Bilotti, O. Fenwick and C. B. Nielsen, *Front. Electron. Mater.*, 2021, **1**, 677845.
23 C. Manjunatha, M. Rafiq, R. Hari Kirshna, S. Nayak, N. Yashaswini, L. Suraj, M. Selvaraj, V. Chaudhary and A. Khosla, *Mater. Res. Innovations*, 2022, 1–14, DOI: 10.1080/14328917.2022.2140784.
24 W.-Y. Chen, X.-L. Shi, J. Zou and Z.-G. Chen, *Mater. Sci. Eng., R*, 2022, **151**, 100700.
25 T. Cao, X.-L. Shi and Z.-G. Chen, *Prog. Mater. Sci.*, 2023, **131**, 101003.
26 Z.-H. Zheng, X.-L. Shi, D.-W. Ao, W.-D. Liu, M. Li, L.-Z. Kou, Y.-X. Chen, F. Li, M. Wei, G.-X. Liang, P. Fan, G. Q. Lu and Z.-G. Chen, *Nat. Sustainability*, 2023, **6**, 180–191.
27 Q. Zhang, K. Deng, L. Wilkens, H. Reith and K. Nielsch, *Nat. Electron.*, 2022, **5**, 333–347.
28 A. C. Ferrari, F. Bonaccorso, V. Fal'ko, K. S. Novoselov, S. Roche, P. Bøggild, S. Borini, F. H. L. Koppens, V. Palermo, N. Pugno, J. A. Garrido, R. Sordan, A. Bianco, L. Ballerini, M. Prato, E. Lidorikis, J. Kivioja, C. Marinelli, T. Ryhänen, A. Morpurgo, J. N. Coleman, V. Nicolosi, L. Colombo, A. Fert, M. Garcia-Hernandez, A. Bachtold, G. F. Schneider, F. Guinea, C. Dekker, M. Barbone, Z. Sun, C. Galiotis, A. N. Grigorenko, G. Konstantatos, A. Kis, M. Katsnelson, L. Vandersypen, A. Loiseau, V. Morandi, D. Neumaier, E. Treossi, V. Pellegrini, M. Polini, A. Tredicucci, G. M. Williams, B. Hee Hong, J.-H. Ahn, J. Min Kim, H. Zirath, B. J. van Wees, H. van der Zant, L. Occhipinti, A. Di Matteo, I. A. Kinloch, T. Seyller, E. Quesnel, X. Feng, K. Teo, N. Rupesinghe, P. Hakonen, S. R. T. Neil, Q. Tannock, T. Löfwander and J. Kinaret, *Nanoscale*, 2015, **7**, 4598–4810.
29 P.-a Zong, J. Liang, P. Zhang, C. Wan, Y. Wang and K. Koumoto, *ACS Appl. Energy Mater.*, 2020, **3**, 2224–2239.
30 A. S. Nissimagoudar and N. S. Sankeshwar, *Phys. Rev. B: Condens. Matter Mater. Phys.*, 2014, **89**, 235422.
31 N. S. Sankeshwar, S. S. Kubakaddi and B. G. Mulimani, in *Advances in Graphene Science*, ed. A. Mahmood, IntechOpen, Rijeka, 2013, ch. 9, pp. 217–271.
32 R. Mulla and C. W. Dunnill, *Compos. Commun.*, 2020, **20**, 100345.
33 Q.-Y. Li, T. Feng, W. Okita, Y. Komori, H. Suzuki, T. Kato, T. Kaneko, T. Ikuta, X. Ruan and K. Takahashi, *ACS Nano*, 2019, **13**, 9182–9189.
34 R. Mulla and M. H. K. Rabinal, *Energy Technol.*, 2019, **7**, 1800850.
35 M. R. Burton, S. Mehraban, D. Beynon, J. McGettrick, T. Watson, N. P. Lavery and M. J. Carnie, *Adv. Energy Mater.*, 2019, **9**, 1900201.
36 C.-J. Yao, H.-L. Zhang and Q. Zhang, *Polymers*, 2019, **11**, 107.
37 Y. Zhang, Q. Zhang and G. Chen, *Carbon Energy*, 2020, **2**, 408–436.
38 W. Chen, P. Xiao, H. Chen, H. Zhang, Q. Zhang and Y. Chen, *Adv. Mater.*, 2019, **31**, 1802403.
39 W. Zhao, S. Fan, N. Xiao, D. Liu, Y. Y. Tay, C. Yu, D. Sim, H. H. Hng, Q. Zhang, F. Boey, J. Ma, X. Zhao, H. Zhang and Q. Yan, *Energy Environ. Sci.*, 2012, **5**, 5364–5369.
40 C. Gayner and K. K. Kar, *Prog. Mater. Sci.*, 2016, **83**, 330–382.
41 I. S. Protsak, S. Champet, C.-Y. Chiang, W. Zhou, S. R. Popuri, J.-W. G. Bos, D. K. Misra, Y. M. Morozov and D. H. Gregory, *ACS Omega*, 2019, **4**, 6010–6019.
42 M. Li, D. L. Cortie, J. Liu, D. Yu, S. M. K. N. Islam, L. Zhao, D. R. G. Mitchell, R. A. Mole, M. B. Cortie, S. Dou and X. Wang, *Nano Energy*, 2018, **53**, 993–1002.
43 Y. Lin, C. Norman, D. Srivastava, F. Azough, L. Wang, M. Robbins, K. Simpson, R. Freer and I. A. Kinloch, *ACS Appl. Mater. Interfaces*, 2015, **7**, 15898–15908.
44 D. Srivastava, C. Norman, F. Azough, D. Ekren, K. Chen, M. J. Reece, I. A. Kinloch and R. Freer, *J. Mater. Chem. A*, 2019, **7**, 24602–24613.
45 P.-a Zong, X. Chen, Y. Zhu, Z. Liu, Y. Zeng and L. Chen, *J. Mater. Chem. A*, 2015, **3**, 8643–8649.
46 B. T. McGrail, A. Sehirlioglu and E. Pentzer, *Angew. Chem., Int. Ed.*, 2015, **54**, 1710–1723.
47 Y.-Y. Hsieh, Y. Zhang, L. Zhang, Y. Fang, S. N. Kanakaraaj, J.-H. Bahk and V. Shanov, *Nanoscale*, 2019, **11**, 6552–6560.
48 H. Wang and C. Yu, *Joule*, 2019, **3**, 53–80.
49 O. Bubnova and X. Crispin, *Energy Environ. Sci.*, 2012, **5**, 9345–9362.
50 Y. Chen, Y. Zhao and Z. Liang, *Energy Environ. Sci.*, 2015, **8**, 401–422.
51 Y. Du, J. Chen, Q. Meng, J. Xu, J. Lu, B. Paul and P. Eklund, *Adv. Electron. Mater.*, 2020, **6**, 2000214.

52 Y. Du, J. Xu, B. Paul and P. Eklund, *Appl. Mater. Today*, 2018, **12**, 366–388.
53 X. Liu, X.-L. Shi, L. Zhang, W.-D. Liu, Y. Yang and Z.-G. Chen, *J. Mater. Sci. Technol.*, 2023, **132**, 81–89.
54 R. Nayak, P. Shetty, M. Selvakumar, A. Rao, K. M. Rao, K. Gurukrishna and S. Mangavati, *J. Alloys Compd.*, 2022, **922**, 166298.
55 G. H. Kim, D. H. Hwang and S. I. Woo, *Phys. Chem. Chem. Phys.*, 2012, **14**, 3530–3536.
56 J. Azadmanjiri, V. K. Srivastava, P. Kumar, M. Nikzad, J. Wang and A. Yu, *J. Mater. Chem. A*, 2018, **6**, 702–734.
57 L. Wang, Q. Yao, H. Bi, F. Huang, Q. Wang and L. Chen, *J. Mater. Chem. A*, 2015, **3**, 7086–7092.
58 B. Abad, I. Alda, P. Díaz-Chao, H. Kawakami, A. Almarza, D. Amantia, D. Gutierrez, L. Aubouy and M. Martín-González, *J. Mater. Chem. A*, 2013, **1**, 10450–10457.
59 M. He, F. Qiu and Z. Lin, *Energy Environ. Sci.*, 2013, **6**, 1352–1361.
60 L. Wang, Q. Yao, H. Bi, F. Huang, Q. Wang and L. Chen, *J. Mater. Chem. A*, 2014, **2**, 11107–11113.
61 T. Ube, J. Koyanagi, T. Kosaki, K. Fujimoto, T. Yokozeki, T. Ishiguro and K. Nishio, *J. Mater. Sci.*, 2019, **54**, 3904–3913.
62 F. Greuter and G. Blatter, *Semicond. Sci. Technol.*, 1990, **5**, 111–137.
63 S. H. Zaferani, R. Ghomashchi and D. Vashaee, *ACS Appl. Energy Mater.*, 2021, **4**, 3573–3583.
64 G. Dennler, R. Chmielowski, S. Jacob, F. Capet, P. Roussel, S. Zastrow, K. Nielsch, I. Opahle and G. K. H. Madsen, *Adv. Energy Mater.*, 2014, **4**, 1301581.
65 E. Muchuweni and E. T. Mombeshora, *Renewable Energy Focus*, 2023, **45**, 40–52.
66 P. Sharief, B. Madavali, S. H. Song, J. K. Lee, K. B. Kim, J. T. Kim, D. H. Kim, J.-H. Han and S.-J. Hong, *Mater. Chem. Phys.*, 2021, **266**, 124512.
67 M. S. Islam, H. Ohmagari, M. A. Rahman, Y. Shudo, M. Fukuda, J. Yagyu, Y. Sekine, L. F. Lindoy and S. Hayami, *Mater. Adv.*, 2021, **2**, 5645–5649.
68 Q. Hu, Y. Zhang, Y. Zhang, X.-J. Li and H. Song, *J. Alloys Compd.*, 2020, **813**, 152204.
69 H. Wang, X. Liu, Z. Zhou, H. Wu, Y. Chen, B. Zhang, G. Wang, X. Zhou and G. Han, *Acta Mater.*, 2022, **223**, 117502.
70 L. Zhao, S. M. K. N. Islam, J. Wang, D. L. Cortie, X. Wang, Z. Cheng, J. Wang, N. Ye, S. Dou, X. Shi, L. Chen, G. J. Snyder and X. Wang, *Nano Energy*, 2017, **41**, 164–171.
71 X. Chen, H. Zhang, Y. Zhao, W.-D. Liu, W. Dai, T. Wu, X. Lu, C. Wu, W. Luo, Y. Fan, L. Wang, W. Jiang, Z.-G. Chen and J. Yang, *ACS Appl. Mater. Interfaces*, 2019, **11**, 22457–22463.
72 A. Dey, S. Hadavale, M. A. S. Khan, P. More, P. K. Khanna, A. K. Sikder and S. Chattopadhyay, *Dalton Trans.*, 2015, **44**, 19248–19255.
73 A. Dey, S. Panja, A. K. Sikder and S. Chattopadhyay, *RSC Adv.*, 2015, **5**, 10358–10364.
74 M. Li, S. M. Kazi Nazrul Islam, S. Dou and X. Wang, *J. Alloys Compd.*, 2018, **769**, 59–64.
75 J. Dong, W. Liu, H. Li, X. Su, X. Tang and C. Uher, *J. Mater. Chem. A*, 2013, **1**, 12503–12511.
76 L. Huang, J. Lu, D. Ma, C. Ma, B. Zhang, H. Wang, G. Wang, D. H. Gregory, X. Zhou and G. Han, *J. Mater. Chem. A*, 2020, **8**, 1394–1402.
77 B. Feng, J. Xie, G. Cao, T. Zhu and X. Zhao, *J. Mater. Chem. A*, 2013, **1**, 13111–13119.
78 A. Bhardwaj, A. K. Shukla, S. R. Dhakate and D. K. Misra, *RSC Adv.*, 2015, **5**, 11058–11070.
79 D. Zhao, X. Wang and D. Wu, *Crystals*, 2017, **7**, 71.
80 D. Suh, S. Lee, H. Mun, S.-H. Park, K. H. Lee, S. Wng Kim, J.-Y. Choi and S. Baik, *Nano Energy*, 2015, **13**, 67–76.
81 M. S. El-Asfoury, M. N. A. Nasr, K. Nakamura and A. Abdel-Moneim, *J. Alloys Compd.*, 2018, **745**, 331–340.
82 X. Feng, Y. Fan, N. Nomura, K. Kikuchi, L. Wang, W. Jiang and A. Kawasaki, *Carbon*, 2017, **112**, 169–176.
83 D. Chen, Y. Zhao, Y. Chen, B. Wang, H. Chen, J. Zhou and Z. Liang, *ACS Appl. Mater. Interfaces*, 2015, **7**, 3224–3230.
84 C. Li, X. Qin, Y. Li, D. Li, J. Zhang, H. Guo, H. Xin and C. Song, *J. Alloys Compd.*, 2016, **661**, 389–395.
85 C. Wu, J. Li, Y. Fan, J. Xing, H. Gu, Z. Zhou, X. Lu, Q. Zhang, L. Wang and W. Jiang, *J. Alloys Compd.*, 2019, **786**, 884–893.
86 Y. Sonvane, S. K. Gupta, P. Raval, I. Lukačević and P. B. Thakor, *Chem. Phys. Lett.*, 2015, **634**, 16–19.
87 J. Chen and B. Liu, *Eur. Phys. J. Plus*, 2021, **136**, 379.
88 R. Mulla, D. R. Jones and C. W. Dunnill, *Adv. Mater. Technol.*, 2020, **5**, 2000227.
89 H. J. Hwang, S.-Y. Kim, S. K. Lee and B. H. Lee, *Carbon*, 2023, **201**, 467–472.